

Institute of Physics, M. Curie-Skłodowska University,
20-031 Lublin, pl. M. Curie-Skłodowskiej 1, Poland

ANDRZEJ BARAN

Nuclear Level Densities in Hartree-Fock-Bogoliubov Model

Gęstości poziomów jądrowych w modelu Hartree-Focka-Bogoliubova

1. INTRODUCTION

Level densities play an important role in an emission of photons, which is a way of deexcitation of nuclear states populated in fusion reactions or deep inelastic processes. Gamma spectrum — the number of photons vs. γ transition energy — shows the exponential tail at high transition energies and a characteristic bump on the top of the exponential dependence [1, 2] at low energies. The exponential part reveals its statistical origin while the bump is the result of the collective rotational gamma transitions. We try to understand the origin of such a spectrum in a framework of microscopic model of the total nuclear level densities.

An interesting effect can also be observed in a side feeding spectra [3]. The side feeding spectrum is a dependence of the number of statistical photons which fall down onto the yrast line¹ on angular momentum (see Fig. 1). The existence of two bumps in this kind of spectra for some nuclei cannot be explained away with statistical (Fermi model) level densities and constant γ -transition probabilities of $E1$, $E2$ and $M1$ transitions. In γ -deexcitation models, which have been already proposed [4–9] latter assumptions are very

¹ The yrast line corresponds to the lowest energy at a given angular momentum.

common. The model which incorporates the energy dependent and angular momentum dependent level densities to the gamma transition probabilities have not been proposed yet.

A procedure which describes the gamma transitions is usually based on the level densities calculated from the partition function [10] or analytical summation of levels [11]. There are also many modifications of the saddle point method (see e.g. [12]). The final density expression obtained from such a procedure is relatively simple and it allows to speed up huge numerical codes calculating the nuclear reactions. An analytical formula obtained for the density $\rho(E, I)$ makes these codes very effective. However, simple, single particle nuclear models and statistical nuclear level density distributions lead to many physical inaccuracies. It is especially true for low energy calculations (≤ 5 MeV) where the important role is played by the discrete spectrum. The standard statistical density curve $\rho(E, I)$ does not account for these discrete levels.

The same can be said about transition probabilities which regulate the cascade calculations. Transition probabilities are treated usually as a free parameters of the model. In this way one has a possibility to simulate real transitions by fitting. On the other hand, there is no insight into the real nature of the gamma deexcitation process of the nucleus in question.

Therefore, in the presented paper we propose a method of calculating level densities in the range of small excitation energies ($E_{exc} < 7 - 8$ MeV above the yrast line) and a method of estimating transition probabilities. As a basis serves fairly realistic nuclear model which describes at a time the collective properties (transitions along yrast line) in a satisfactory way. The statistical γ -transitions above the yrast line are extracted from the properties of excited states.

In the following we apply a Hartree-Fock-Bogoliubov (HFB) procedure to the Hamiltonian of the Pairing plus Quadrupole-Quadrupole (P+QQ) type [13–15]. This is a foundation of calculating both the level density and matrix elements of transition operators.

A description of the method is presented in the following chapter. Nuclei with large angular momentum are described in the Bogoliubov picture by the method of Mang et al. [15–17]. In the second part of this paper we shortly present the HFB procedure and describe the method of solution of the problem of projection on a good angular momentum space and the good number of particles. The third part of the paper shows the way of calculating the density of levels. In the last part of the paper we shall show results for calculated level densities and we shall discuss some consequences of gamma deexcitation process. Gamma spectra, side feeding pattern and multiplicities

of different gamma modes are compared to the old fashion calculations which include the Fermi type of the level densities. The differences between these two types of calculations seem to validate the method of level counting scheme performed in the present paper.

2. HARTREE-FOCK-BOGOLIUBOV METHOD

In this section we briefly describe the HFB procedure. Let

$$\hat{H} = \sum_{kl} \epsilon_{kl} c_k^\dagger c_l + \sum_{klmn} V_{klmn} c_k^\dagger c_l^\dagger c_n c_m \quad (1)$$

be the Hamiltonian operator of the nuclear system, where ϵ_{kl} is a single particle kinetic energy matrix element, V is a two body interaction, and c, c^\dagger are annihilation and creation operators of nucleons. The Bogoliubov transformation is a transformation from the particle basis $\{c\}$ to the basis of quasiparticles $\{\alpha\}$:

$$\alpha_k^\dagger = \sum_k U_{lk} c_l^\dagger + V_{lk} c_l. \quad (2)$$

The operators $\{\alpha\}$ have the same commutation properties as original particle operators $\{c\}$.

The transformation given by Eq. (2) does not preserve the symmetries of the Hamiltonian. The particle number as well as the angular momentum are no longer conserved in the considered system. The particle number can be approximately restored through the introduction of the chemical potential λ and passage to the new Hamiltonian

$$\hat{H}_\lambda = \hat{H} - \lambda \hat{N}. \quad (3)$$

The Lagrange parameter λ is determined from the condition

$$\langle \hat{N} \rangle = N, \quad (4)$$

where $\langle \hat{N} \rangle$ is the expectation value of the particle number operator \hat{N} , and N is the number of particles in the system. After the transformation given by Eq. (2) the Hamiltonian takes the form

$$\hat{H} = H^{00} + \hat{H}^{11} + \hat{H}^{20} + \hat{H}_{int}, \quad (5)$$

where superscripts (km) correspond to linear combinations of the products of quasiparticle operators and indicate the number of creation (k) and annihilation (l) operators, e.g.

$$\hat{H}^{20} = \sum_{kl} H_{kl}^{20} \alpha_k^\dagger \alpha_l^\dagger + h.c. \quad (6)$$

Here, the matrix H^{20} is

$$H^{20} = U^\dagger h V^* - V^\dagger h^T U^* + U^T \Delta U^* - V^T \Delta^* V^*, \quad (7)$$

and matrices h and Δ are given by

$$h = \epsilon + \Gamma, \quad (8a)$$

$$\Gamma_{lm} = \sum_{pq} V_{lqm} \rho_{pq}, \quad (8b)$$

$$\Delta_{lm} = \frac{1}{2} \sum_{pq} V_{lmpq} \kappa_{pq}, \quad (8c)$$

$$\rho = V^* V^T, \quad (8d)$$

$$\kappa = V^* U^T. \quad (8e)$$

In all these formulas U and V are the transformation matrices whose matrix elements appear in Eq. (2), ρ is a density matrix, κ is a pairing tensor and h and Γ are the self consistent single particle energy and the potential respectively. The matrix Δ is a self consistent pairing potential.

The wave function of the nuclear system is determined from the following variation of an expectation value of the energy

$$\delta \frac{\langle \phi | \hat{H} | \phi \rangle}{\langle \phi | \phi \rangle} = 0. \quad (9)$$

To solve this variational problem one uses Thoules theorem and the gradient method (see e.g. ref. [17]).

A wave function $|\phi'\rangle = |\phi\rangle + |\delta\phi\rangle$ is assumed to have the form

$$|\phi'\rangle = \exp\left\{ \sum_{k(l)} Z_{kl} \alpha_k^\dagger \alpha_l^\dagger \right\} |\phi\rangle, \quad (10)$$

where $Z_{kl}(k(l))$ are independent variables. The solution of the variational problem (9) corresponds to $Z_{kl} = 0$. The equation (9) reduces to the condition

$$\frac{\partial}{\partial Z_{kl}} \frac{\langle \phi' | \hat{H} | \phi' \rangle}{\langle \phi' | \phi' \rangle} = \hat{H}_{kl}^{20} = 0. \quad (11)$$

Both, this condition and a diagonalization of the \hat{H}^{11} part of the Hamiltonian determine completely Bogoliubov transformation matrices V, U . The Hamiltonian takes the form

$$\hat{H}_\lambda = H^0 + \sum_k E_k \alpha_k^\dagger \alpha_k + \hat{H}_{int}, \quad (12)$$

where \hat{H}_{int} contains terms $\hat{H}^{22}, \hat{H}^{31}, \hat{H}^{40}$, which will be neglected in the HFB approach; E_k is a quasiparticle energy.

Eigenstates of \hat{H}_λ are, a quasiparticle vacuum $|\phi\rangle$ — this belongs to the lowest eigenvalue $E_0 = H^0$, one quasiparticle state

$$|\phi_k\rangle = \alpha_k^\dagger |\phi\rangle, \quad (13)$$

belonging to eigenvalue E_k , two quasiparticle states $\alpha_k^\dagger \alpha_l^\dagger |\phi\rangle$ etc. Generally, n -quasiparticle state² can be written in the form

$$|\{n\}\rangle = \alpha_{k_1}^\dagger \dots \alpha_{k_n}^\dagger |\phi\rangle. \quad (14)$$

Its energy (the eigenvalue of \hat{H}_λ) measured relatively to the ground state energy is equal to

$$E_{\{n\}} = E_{k_1} + E_{k_2} + \dots + E_{k_n}. \quad (15)$$

In order to simplify the problem we shall use a phenomenological Hamiltonian which accounts for deformation and short range correlations among particles. The simplest and effective model is e.g., the P+QQ model suggested by Bohr and Mottelson and widely viewed by Kumar and Baranger [13-15]. The Hamiltonian of this model has the form

$$\hat{H} = \sum_k \epsilon_k c_k^\dagger c_k - \frac{\chi}{2} \sum_\mu \hat{Q}_\mu^\dagger \hat{Q}_\mu - G \hat{P}^\dagger \hat{P}, \quad (16)$$

where the quadrupole operator \hat{Q}_μ reads

$$\hat{Q}_\mu = \sum_{kl} \langle k|r^2 Y_{2\mu}|l\rangle c_k^\dagger c_l \quad (17)$$

and the pairing operator

$$\hat{P}^\dagger = \sum_{k)0} c_k^\dagger c_{\bar{k}}^\dagger. \quad (18)$$

² In the following we consider only even n quasiparticle excitations. The odd n excitations belong to the odd nuclear systems.

Here bar over k (\bar{k}) denotes the time reversal operation on the state k . Constants χ and G as well as single particle energies ϵ_k depend on the configuration space and are adjusted from an experimental data. A linearization of the Hamiltonian (16) which corresponds to the Hartree-Fock prescription (average field approximation) yields

$$\hat{H}_{HFB} = \sum_k \epsilon_k c_k^\dagger c_k - \frac{\chi}{2} \sum_\mu q_\mu (\hat{Q}_\mu^\dagger + \hat{Q}_\mu) - p_0 (\hat{P}^\dagger + \hat{P}), \quad (19)$$

where

$$q_\mu = \chi \langle \phi | Q_\mu | \phi \rangle, \quad (20)$$

and

$$p_0 = G \langle \phi | \hat{P} | \phi \rangle. \quad (21)$$

As we said before, rotational and particle number symmetries are broken by Bogoliubov transformation. In order to restore these symmetries at least partly, one can use the variational procedure (Eq. 9) in case of a new Hamiltonian

$$\hat{H}_c = \hat{H} - \lambda \hat{N} - \omega \hat{I}_x. \quad (22)$$

The variational problem becomes

$$\delta \langle \phi_\omega | \hat{H}_c | \phi_\omega \rangle = 0. \quad (23)$$

The Lagrange multiplier ω is connected to the angular momentum I of the system through the constraint

$$\langle \phi_\omega | \hat{I}_x | \phi_\omega \rangle = \sqrt{I(I+1)}. \quad (24)$$

Here $|\phi_\omega\rangle$ are internal wave functions. The operator \hat{I}_x breaks the time reversal symmetry as well. Therefore, time reversal conjugate states \bar{k} of the system are not known. The variational procedure leads to the extended HFB equations in the rotating frame. These are

$$\begin{pmatrix} h - \omega \hat{j}_x & \Delta \\ -\Delta^* & -h + \omega \hat{j}_x \end{pmatrix} \begin{pmatrix} U_k \\ V_k \end{pmatrix} = E_k \begin{pmatrix} U_k \\ V_k \end{pmatrix}. \quad (25)$$

Here \hat{j}_x denotes the x -component of the single particle angular momentum operator.

The variation (23) performed at a given angular momentum I leads to the lowest energy (*yrast state*) and allows to extract the sequence of single quasiparticle energies E_k ($k = 1, 2, 3, \dots$) corresponding to the rotational

state I . Quasiparticles will contribute to the total level densities of the nucleus.

The conservation of average number of particles and the angular momentum corrects the energy spectrum of the system. The complete restoration of the symmetries broken in Bogoliubov transformation can be achieved through the application of the projection operators \hat{P}^I and \hat{P}^N to the wave function $|\phi_\omega\rangle$. These operators project onto the good angular momentum space and particle number respectively. The projected wave function is given by

$$\psi^{NIM} = \sum_k g_k \hat{P}_{MK}^I \hat{P}^N |\phi\rangle. \quad (26)$$

Explicit forms of the projection operators are

$$\hat{P}^N = (2\pi)^{-1} \int_0^\pi e^{i\varphi(\hat{N}-N)} d\varphi, \quad (27)$$

and

$$\hat{P}_{MK}^I = \frac{(2I+1)}{8\pi^2} \int D_{MK}^{I*}(\Omega) \hat{R}(\Omega) d\Omega. \quad (28)$$

Here, quantities D_{MK}^I are the Wigner matrices and $\hat{R}(\Omega)$ is the operator of rotation on the angle Ω . Coefficients g_k in Eq. (26) should be determined by the solution of the generalized eigenvalue problem (variation before projection method — VBP or projection after variation — PAV)

$$\sum_{K'} h_{KK'}^I g_{K'} = E^I \sum_{K'} n_{KK'}^I g_{K'}, \quad (29)$$

where

$$h_{KK'}^I = \langle \phi | \hat{H} \hat{P}_{KK'}^I | \phi \rangle, \quad (30)$$

$$n_{KK'}^I = \langle \phi | \hat{P}_{KK'}^I | \phi \rangle, \quad (31)$$

or from the equations

$$\sum_{K'} g_{K'} \langle \phi | (\hat{H} - E^I) \hat{P}_{KK'}^I | \phi \rangle = 0, \quad (32)$$

$$\sum_{KK'} g_K^* g_{K'} \langle \delta\phi | (\hat{H} - E^I) \hat{P}_{KK'}^I | \phi \rangle = 0, \quad (33)$$

(variation after projection, VAP). If we decompose $|\phi\rangle$ into the internal K -components then

$$\psi^{NIM} = \hat{P}^N \sum_K \hat{P}_{MK}^I \sum_{K'} g_{K'} |\phi_{K'}\rangle = \hat{P}^N \sum_K \hat{P}_{MK}^I |\tilde{\phi}\rangle. \quad (34)$$

The function

$$|\tilde{\phi}\rangle = \sum_K g_K |\phi_K\rangle \quad (35)$$

is not in general a product wave function but in many cases it can be approximated by a function of this type. An example is e.g. the function $|\phi\rangle$ which has only slightly different symmetry than the axially symmetric wave function. In what follows we assume a symmetry of this type. This approximation allows to use the Kamlah's angular momentum projection operator \hat{P}_M^I [17, 18]:

$$\hat{P}_M^I = \sum_K \hat{P}_{MK}^I. \quad (36)$$

This operator simplifies all the calculations and conserves the features of the considered deformed system [17]. The total projected wave function is given by

$$\psi^{NIM} = P^N \sum_K \hat{P}_{MK}^I |\phi\rangle = \hat{P}^N \hat{P}_M^I |\phi\rangle. \quad (37)$$

We shall use this formula in derivations of gamma transition probabilities. The quasiparticle energies which we calculate in the following are obtained in the VAP method [17, 15].

3. LEVEL DENSITIES

In a model of noninteracting fermions the level density is equal to the number of ways in which the nucleons can be distributed among available single-particle (or single-quasiparticle) levels at a fixed total energy of the whole system.

There are two ways to determine the densities of energy levels: a) the spectroscopical approach applied in the case of low energy levels and b) the statistical approach in the case of high energy excited systems. Methods applied at low energies give usually the yrast states or a low vibrational states. At intermediate and high energies one can use temperature dependent models [19, 20]. In real cases statistical calculations become too complex and can be performed only within a help of huge computers. In simpler cases there are used combinatorial methods which are suggested by the definition of the level density. Calculations of this type have been performed by Hillman and Grover [22] and by Gilat [23]. In these approaches the nuclear levels are counted exactly one by one. The disadvantage arises from the large values which the level density can reach (typically 10^6 MeV at

the neutron binding energy). Calculations have to be highly sophisticated in order to manage successfully with this problem.

If the level density is expected to be high, the partition function method becomes effective and it is widely used. In the case of noninteracting systems of particles, like protons and neutrons³, the partition function \mathcal{Z} can be written as the product of partition functions of subsystems [24]

$$\mathcal{Z} = \mathcal{Z}_Z \mathcal{Z}_N, \quad (38)$$

where \mathcal{Z}_Z and \mathcal{Z}_N are partition functions for protons and neutrons respectively. The formula for the partition function \mathcal{Z} , e.g. for neutrons, reads

$$\mathcal{Z}_N(\alpha, \beta) = \sum_{N'} \int dE' \rho(E', N') \exp(\alpha_N N' - \beta E'). \quad (39)$$

A total partition function \mathcal{Z} of the system is

$$\mathcal{Z} = \sum_{N', Z'} \int dE' \rho(E', N', Z') \exp(\alpha_N N' - \alpha_Z Z' - \beta E'). \quad (40)$$

This determines the total density $\rho(U, N, Z)$ of the system. The total density is the convolution of both $\rho(E, N)$ and $\rho(E, Z)$

$$\rho(U, N, Z) = \int_0^U \rho(E, N) \rho(U - E, Z) dE. \quad (41)$$

It follows from this expression that the densities of protons and neutrons separately determine the density of states of the whole $(N + Z)$ -system.

In the presented paper we used the formula (41) and a combinatorial procedure based on quasiparticle levels obtained from the P+QQ model described in section II.

As we have seen, the particle number and the angular momentum in the HFB model are not conserved. This influences the calculated level densities. In order to correct the total number of levels (usually too large) one needs feasible methods of both projection on angular momentum and particle number in the case of excited states. Methods which we have described before and which are based on projection techniques lead to too slow numerical procedures. Therefore these methods can be used only at very low energies where the number of levels is small.

³ The assumption on noninteracting protons and neutrons is typical in shell models and is valid at specific conditions — the single particle potentials for protons and neutrons are different.

In order to understand better the overcounting problem I shall illustrate it in an example. To see that the number of levels calculated in procedures of adding them up, is usually larger than in the reality let us consider a special case of the nucleus in its ground state which is a pure Hartree-Fock state. The only excitations which are physically possible in this case are these in which the number of particles is equal to the number of holes. Since the transformation from particles to quasiparticles mixes both creation and annihilation operators with different ratios, the conservation of particles and holes is not fulfilled in the quasiparticle approximation. The total number of nuclear levels based on many quasi-particle excitations is larger than the number of levels in which number of holes and particles are the same.

In order to correct the mistaken densities we follow two simple methods. The first method is adapted from Bohr-Mottelson handbook [25]. Consider the fluctuations in the particle number associated with the simple quasiparticle spectrum. Let the occupation function f be

$$f = (1 + \exp \beta E_\nu)^{-1}. \quad (42)$$

In the excited physical state the number of holes $n(h)$ equals to the number of particles $n(p)$. Using the expectation values one has

$$\langle n(p) - n(h) \rangle = 0, \quad (43)$$

and

$$\langle [n(p) - n(h)]^2 \rangle = g_0 \beta^{-1}, \quad (44)$$

Here g_0 is the level density at the Fermi energy of the considered system. The distribution of the difference $\Delta = n(p) - n(h)$ is Gaussian since in any given state, Δ is the algebraic sum of many independent contributions from the different single particle states. Therefore, the normalized distribution function of Δ is

$$P(\Delta) = (2\pi g_0 \beta^{-1})^{-1/2} \exp\left(-\frac{\Delta^2}{2g_0 \beta^{-1}}\right). \quad (45)$$

From this we learn that the probability for the state to be physical corresponding to $\Delta = 0$ is

$$P(0) = (24g_0 E)^{-1/4}. \quad (46)$$

It follows that the density calculated on the basis of quasiparticle excitations have to be corrected on a factor of $(24g_0 E)^{-1/4}$. In this way one removes the fraction of spurious states for which the total number of particles is different

as compared to ground state. We may say that $P(\Delta = 0)$ corrects for states whose have the number of particles and holes equal.

The second method of correcting the nuclear spectrum is purely numerical and is performed in the following way. For each excited n -quasiparticles state $|\{n\}\rangle$, the average value of the neutron (or proton) number is determined numerically and the state is *rejected* in the levels counting procedure if $|\langle \hat{N} \rangle - N| > 1/2$. Here N is the number of particles. As it was shown elsewhere [26] this procedure gives results comparable to those obtained from the previous method.

The analogous procedure was applied to correct the density with respect to angular momentum. According to Hartree-Fock-Bogoliubov model only those states are counted for which the x -component of angular momentum is *approximately* conserved (i.e. it is the same as in the ground state). We assumed that the difference between both the ground state angular momentum $\langle \hat{I}_x \rangle_0$ and the angular momentum of excited state $\langle \hat{I}_x \rangle_{\text{exc}}$ is less than 1/2. In the ground state

$$\langle \hat{I}_x \rangle_0 = \sqrt{I(I+1)}. \quad (47)$$

For an excited state one gets

$$\langle \hat{I}_x \rangle_{\text{exc}} = \langle \{n\} | \hat{I}_x | \{n\} \rangle = \sum_i' (I_x^{11})_{ii} + \sqrt{I(I+1)} = \sum_i' \langle i | \hat{j}_x | i \rangle + \sqrt{I(I+1)}. \quad (48)$$

Here the summation in this formula runs only over excited single particle orbitals. According to our assumption

$$\delta_I = |\langle \hat{I}_x \rangle_{\text{exc}} - \langle \hat{I}_x \rangle_0| = \left| \sum_i' \langle i | \hat{j}_x | i \rangle \right| < 1/2. \quad (49)$$

Both corrections on particle number and on angular momentum diminish the originally counted density on a factor of 10–15 [26].

4. TRANSITION PROBABILITIES

The probability of the gamma transition used in cascade calculations is given by the following formula

$$T(\hat{O}\lambda; i \rightarrow f) = C_{O\lambda}(E_i - E_f)^{2\lambda+1} \rho_f. \quad (50)$$

Here, $|i\rangle = |E_i I_i\rangle$ is the initial state with the energy E_i and the angular momentum I_i , and $|f\rangle = |E_f I_f\rangle$ is the final state of the nucleus correspondingly. A constant $C_{O\lambda}$ refers to the transition operator $\hat{O}\lambda$ of multipolarity λ and ρ_f is the final nuclear level density. The parameters $C_{O\lambda}$ are either estimated from transition strengths between low lying states or are taken as Weisskopf valuations [27]. As a matter of fact $C_{O\lambda}$ have to depend on the angular momenta I_i and I_f as well as energies E_i and E_f . In the following we try to calculate these *constants* from an energy averaged reduced transition probabilities. The latter are estimated from P+QQ nuclear model described in section II.

We follow here the paper by Ring et. al. [28] in which the analogous procedure was applied in the case of yrast transitions. As we said before the ground state or the yrast state $|\phi\rangle$ of the nucleus in a self consistent cranking model is a state violating time reversal, particle number and axial symmetry. The wave function ψ^{IM} with angular momentum I and its third component M can be obtained by projection. I shall use the following approximations:

- i) Calculating the average transition rates we shall restrict the basis to 2qp (two quasiparticle) states. The number of 2qp excitations is already so large that one expects good average values of transition probabilities calculated on the basis of this sub ensemble of states.
- ii) We use the K a m l a h projection technique [17, 18, 28] of zeroth order, in calculations of matrix elements of the transition operators (Eq. 37).
- iii) Calculating the matrix element of the transition operator we take the same Bogoliubov representation for the final and initial states. It means e.g., that we use a given Bogoliubov basis for the yrast state with angular momentum I obtained from the self consistent cranking model and the same basis for the states that can be coupled by the transition operator considered (e.g., states $I - k$, where $k = -\lambda, -\lambda + 1, \dots, \lambda$ for $\hat{O}\lambda$ operator). This procedure is well justified for small λ 's. In our case the maximal λ is equal 2 (in the case of electromagnetic quadrupole transition). The quasiparticles are similar in both considered states.
- iv) We use the asymptotic expansions for the $3 - j$ symbols in the limit $K \ll I$ [29].

The normalized, angular momentum projected wave function $|\psi^{IM}\rangle$ is:

$$|\psi^{IM}\rangle = N_I \sum_K \sum_K \hat{P}_{MK}^I |\{n\}\rangle. \quad (51)$$

The \hat{P}_{MK}^I is the projection operator (27) and N_I is the normalization factor given by

$$N_I^{-2} = \sum_{KM} \langle \{n\} | \hat{P}_{MK}^I | \{n\} \rangle. \quad (52)$$

The reduced transition matrix element of $\hat{O}\lambda$ operator is

$$\begin{aligned} \langle \psi^{I'} | | \hat{O}\lambda | | \psi^I \rangle &= N_I N_{I'} \sum_{KK'\bar{K}\mu} (2I+1)(-)^{I'-K'} \\ &\left(\begin{array}{ccc} I' & \lambda & I \\ -K' & \mu & \bar{K} \end{array} \right) \langle \{n\} | \hat{O}(\lambda\mu) \hat{P}_{KK}^I | \{n\} \rangle. \end{aligned} \quad (53)$$

A similar expression consisting of $\langle \{n\} | P_{K'K}^{I'} \hat{O}(\lambda\mu) | \{n\} \rangle$ on the RHS of the Eq. (53), can be derived. An average of both expressions gives the approximate value of the reduced matrix element $\langle \psi^{I'} | | \hat{O}\lambda | | \psi^I \rangle$ which reads

$$\langle \psi^{I'} | | \hat{O}\lambda | | \psi^I \rangle \approx \sum_{\mu} F(II'\lambda\mu) \sqrt{2I+1} \langle \hat{O}(\lambda\mu) \rangle_{\{n\}} \frac{1}{2} [\chi + \chi^{-1}]. \quad (54)$$

A factor $F(II'\lambda\mu)$ originates from the $3-j$ symbol under the assumption iv). It was shown [28] that the factor χ given by the formula

$$\chi = \chi(II') \equiv N_I (2I+1)^{\frac{1}{2}} / N_{I'} (2I'+1)^{\frac{1}{2}}, \quad (55)$$

if calculated for off-diagonal matrix elements with $I' = I - 2$ is close to unity for yrast states. We adopt this approximation also for excited 2qp states and for all considered angular momenta. The justification of this assumption follows from the fact of the similar structure of both low excited and yrast state. This leads to the expression

$$\langle \psi^{I'} | | \hat{O}\lambda | | \psi^I \rangle \approx \sum_{\mu} F(II'\lambda\mu) \langle 2qp | \hat{O}(\lambda\mu) | 2qp \rangle (2I+1). \quad (56)$$

The next step is the averaging of the reduced transition probability over the final and the initial energies. The procedure follows from the definition of $B(I \rightarrow I'; \hat{O}\lambda)$. The averaging is performed over all final and initial states whose are connected by the operator $\hat{O}\lambda$. In the case of the final yrast states the averaging should be performed with respect to the initial energy interval only. The average value of the reduced transition \bar{B}_{yr} in this case is

$$\bar{B}_{yr}(E, I) = \frac{1}{\Delta\rho_i} \sum B(\hat{O}\lambda; E, I \rightarrow E_{yr}, I_{yr}), \quad (57)$$

where ρ_i is the density of states at the initial energy and angular momentum and Δ is the energy interval in which $B(\hat{O}\lambda; E, I \rightarrow E_{yr}, I_{yr})$ are calculated. Here E_{yr}, I_{yr} are yrast energy and angular momentum respectively. The summation in Eq. (57) runs over all 2qp states whose energies are comprised in the interval Δ . Expanding the transition operator $\hat{O}(\lambda\mu)$ in the quasiparticle basis (see Eq. 2, section II) we get

$$\bar{B}(\hat{O}\lambda; I, E \rightarrow I_{yr} E_{yr}) = \frac{1}{\Delta\rho_i} \sum_{kl} \left| \sum_{\mu} F(I I' \lambda \mu) \mathcal{O}_{kl}^{20}(\lambda\mu) \right|^2. \quad (58)$$

Here $\mathcal{O}_{kl}^{20}(\lambda\mu)$ are the expansion coefficients of the operator \hat{O}^{20} :

$$\hat{O}^{20}(\lambda\mu) = \frac{1}{2} \sum_{kl} [\mathcal{O}_{kl}^{20}(\lambda\mu) \alpha_k^\dagger \alpha_l^\dagger + \mathcal{O}_{lk}^{20}(\lambda\mu) \alpha_l \alpha_k]. \quad (59)$$

The averaging in a non-yrast energy region leads to the formula

$$\bar{B}(\hat{O}\lambda; I_i E_i \rightarrow I_f E_f) = \frac{1}{\Delta_i \Delta_f \rho_i \rho_f} \sum B(\hat{O}\lambda; I_i E_i \rightarrow I_f E_f). \quad (60)$$

The summation runs over all qp-states consisting of the initial state (i) with energy in the interval $I_{E_i} = [E_i - \Delta/2, E_i + \Delta/2]$, and over qp-states consisting of the final state (f) with energy in the interval $I_{E_f} = [E_f - \Delta/2, E_f + \Delta/2]$.

In a 2qp-basis the expression for \bar{B} is

$$\bar{B}(\hat{O}\lambda; I_i E_i \rightarrow I_f E_f) = \frac{1}{\Delta_i \Delta_f \rho_i \rho_f} \sum_{klmnp} \left| \sum_{\mu} F(I_i I_f \lambda \mu) \times \right. \quad (61)$$

$$\left. \times \left(\mathcal{O}^0(\delta_{km} \delta_{ln} - \delta_{lm} \delta_{kn}) + \left(\mathcal{O}_{lm}^{11} \delta_{nk} - \mathcal{O}_{lk}^{11} \delta_{nm} - \mathcal{O}_{mn}^{11} \delta_{lk} + \mathcal{O}_{nk}^{11} \delta_{ml} \right) \right) \right|^2.$$

The \mathcal{O}_{kl}^{11} are the expansion coefficients of \hat{O} in the Bogoliubov basis, e.g.,

$$\hat{O}^{11}(\lambda\mu) = \sum_{kl} \mathcal{O}_{kl}^{11} \alpha_k^\dagger \alpha_l \quad (62)$$

and \mathcal{O}^0 is the diagonal matrix element of \mathcal{O} calculated for two considered excited states. All δ -symbols in Eq. (61) simplify the formula and limit the summations to three indices. The \mathcal{O}^0 part can be separated out of the transition matrix element and it gives the contribution to the collective

transitions which are meaningful in the cascade calculations [7, 26, 30]. The collective part has a form

$$\Delta^2 n \bar{B}_{coll} = \sum_{k>l} |\mathcal{O}_F^0|^2 + 2 \sum_{k>l} \mathcal{O}_F^0 (\mathcal{O}_l^1 + \mathcal{O}_k^1), \quad (63)$$

where

$$\mathcal{O}_l^1 = \sum_{\mu} F(II'\lambda\mu) \mathcal{O}_{ll}^{11}, \quad (64)$$

$$\mathcal{O}_F^0 = \sum_{\mu} F(II'\lambda\mu) \mathcal{O}^0. \quad (65)$$

The factor n on the LHS of Eq. 63 has a meaning of the number of 2qp states passing instantaneously through both the initial and the final energy bins. It may be estimated from a slope of the energy of the 2qp state in the following way. Let E be the energy of the 2qp state. The final energy E' as calculated for the pair of considered quasiparticles is approximately

$$\begin{aligned} E' &= E - (I_f - I_i) \frac{dE}{dI} \\ &= E - (I_f - I_i) \frac{d\omega}{dI} \frac{dE}{d\omega} \\ &= E - \Delta I \cdot \frac{1}{\mathcal{J}} \langle 2qp | \hat{j}_x | 2qp \rangle. \end{aligned} \quad (66)$$

Here \mathcal{J} is a moment of inertia and in the first approximation it equals to the yrast value. If the collective part of the transition operator gives finite contribution to \bar{B}_{coll} and both E and E' are in the initial and final energy bins I_{E_i} and I_{E_f} respectively then the number n (initially set to zero) is increased by 1. By repeating this procedure for all states whose energies are in the initial energy bin it is possible to estimate n .

The procedure described in this chapter can be performed for each transition operator. The result of this is the new transition probability (compare Eq. 50)

$$T(\hat{\mathcal{O}}\lambda; i \rightarrow f) = c_{\lambda} (E_i - E_f)^{2\lambda+1} \bar{B}(\hat{\mathcal{O}}\lambda; I_i E_i \rightarrow I_f E_f) \rho_f, \quad (67)$$

where c_{λ} is now a pure numerical factor depending on the multipolarity λ of gamma radiation [25]

$$c_{\lambda} = \frac{8\pi(\lambda+1)}{\lambda[(2\lambda+1)!!]^2} \frac{1}{\hbar c^{2\lambda+1}}. \quad (68)$$

Both the energy dependence and the spin dependence of the transition probability $T(\hat{\mathcal{O}}\lambda)$ are now included in the level density ρ and in average transition probabilities $\bar{B}(\hat{\mathcal{O}}\lambda, IE \rightarrow I'E')$.

5. RESULTS

In this section we would like to present results of our calculations. We have considered two independent models of level densities, the Fermi model (FM) and the model described in section II. The results of calculations of gamma cascades obtained with both of them are viewed.

On the first series of figures (Figures 1–3) there are shown level densities calculated according to the prescription of section III for the nucleus ^{158}Dy . Figures display the logarithm of level density for spin values $I = 0, 4, 8, 2, 16$ and 20 respectively. There are three different curves shown in each

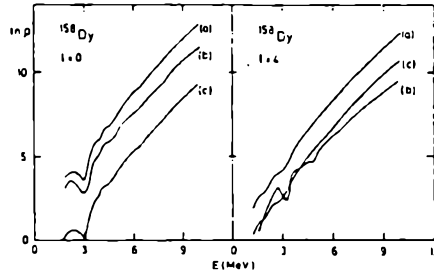


Fig. 1. Level densities of ^{158}Dy for spins $I = 0, I = 4$ as calculated without (a) and with corrections (b, c) as functions of excitation energy. (a) uncorrected, (b) corrected for particle number N and angular momentum conservation I , ($|\Delta j_x| < 1/2$) and (c) corrected for N and multiplied by $|c_I|^2 = \sum_K \langle P_K^K \rangle$

Gęstości poziomów ^{158}Dy dla przypadku stanów $I = 0, I = 4$ wyliczone bez poprawki (a) oraz z poprawkami (b, c) w funkcji energii wzbudzenia. Przypadek (b) zawiera poprawkę na liczbę cząstek N oraz moment pędu I , ($|\Delta j_x| < 1/2$), a przypadek (c) zawiera poprawkę na liczbę cząstek N i uwzględnia czynnik $|c_I|^2 = \sum_K \langle P_K^K \rangle$

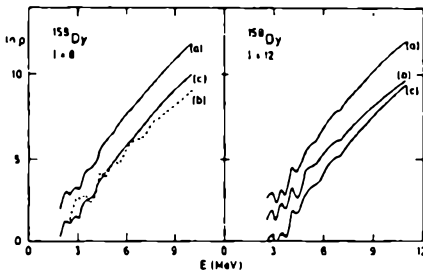


Fig. 2. The same as in Figure 1 but for $I = 8$ i $I = 12$

To samo, co na rycinie 1, lecz dla spinów $I = 8$ i $I = 12$

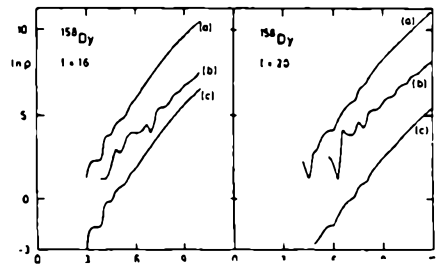


Fig. 3. The same as in Figure 1 but for $I = 16$ and $I = 20$

To samo, co na rycinie 1, lecz dla spinów $I = 16$ i $I = 20$

figure. The curve (a) corresponds to the bar density without particle number and angular momentum corrections. The curve (b) is obtained as a result of a particle number and angular momentum correction according to '1/2' procedure described in section III. The curve (c) is again the particle number and angular momentum corrected level density. The angular momentum correction was performed by multiplying the particle number corrected results by the factor

$$|c_I|^2 = \sum_K \langle P_{KK}^I \rangle. \quad (69)$$

This describes the probability of finding the state with angular momentum I in an actual state $|\rangle$ (see Figure 4 and the discussion of the projection operators in section II). The characteristic feature of all curves displayed is the structure at low energies stretching to approximately 7 MeV. This is the reflection of the single quasi particle (single particle) low energy level structure of the nucleus. It is properly taken into account here through quasiparticle spectra, which are different for different angular momenta. The spectra start at energies equals approximately the gap energy in the pairing interaction. It is worthwhile mentioning that average slopes of density curves are in a good agreement with experimental data.

In Figure 4 we show the exact values of probability distribution of the

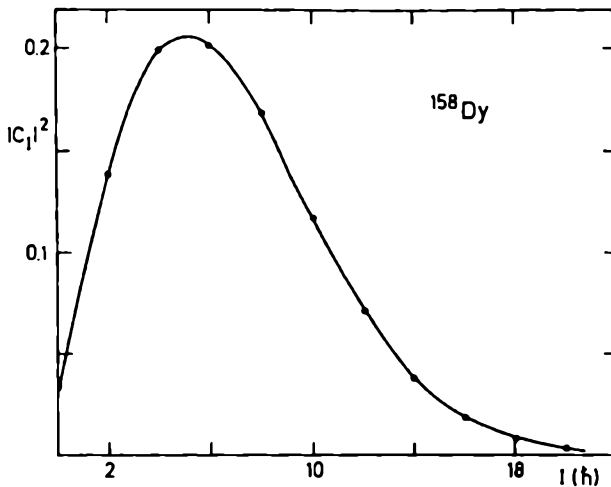


Fig. 4. The $|c_I|^2$ coefficient as a function of I in case of the ground state of ^{158}Dy . The value $|c_{I=0}|^2 \approx 0.03$ gives the probability of finding the state with $I = 0$ in HFB state $|I = 0 \rangle$!

Współczynnik $|c_I|^2$ w funkcji I w przypadku stanu podstawowego jądra ^{158}Dy . Wartość $|c_{I=0}|^2 \approx 0,03$ jest prawdopodobieństwem znalezienia momentu pędu $I = 0$ w stanie HFB $|I = 0 \rangle$!

angular momentum I in the ground state HFB wave function. It is given by the formula (69). One can see that the maximal values of the probability correspond to $I = 4$ and 6 , ($|c_I|^2 = 0.2$) and not to $I = 0$ as might be expected. The distribution is the result of the rotational symmetry breaking by the HFB procedure. Results displayed in Figure 4, influence, as we have mentioned before, the level densities. The value of $|c_0|^2 \approx 0.03$ will modify the calculated (by counting) density value $\rho(E, I = 0)$.

Calculated level densities were used to simulate the gamma cascade process of deexcitation of the ^{158}Dy system. The nucleus was initially excited to the energy of about 10 MeV and to angular momenta distributed as shown in Figure 5. The distribution is the Gaussian, centered at the momentum $I = 28 \hbar$. The shaded area shows the region of angular momenta taken in cascade calculations.

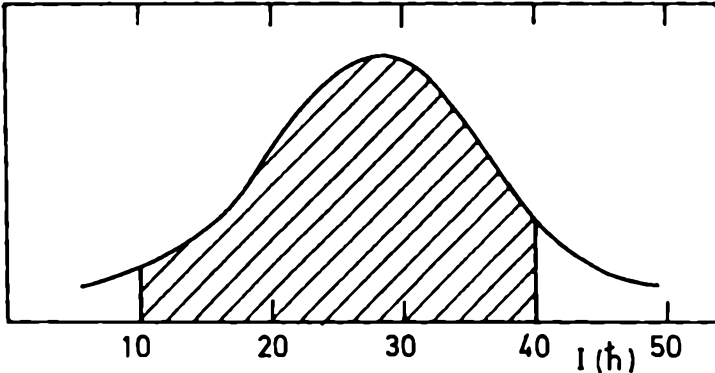


Fig. 5. The shape of initial spin distribution used in cascade calculations
Kształt początkowego rozkładu spinów używanego w obliczeniach

We have compared results of calculations to known, very common phenomenological model based on statistical level densities. We have considered here the Fermi model (FM). The level densities were calculated from the formula given in [25]. In both FM and HFB model we shall consider two separate cases. The first one corresponds to transition rates [7] $C_{E1} : C_{M1} : C_{E2} : C_{E2_{\text{coll}}} = 150 : 25 : 1 : 200$ and the second one to $C_{E1} : C_{M1} : C_{E2} : C_{E2_{\text{coll}}} = 150 : 25 : 1 : 600$. On following figures and in the rest of this paper we refer to them as to ‘200’ and ‘600’ models e.g., FM-600 means Fermi model of the densities with relative collective $E2$ strength equal 600.

The cascade code runs according to the Monte Carlo simulation technique as described e.g., in [31, 32]. The type of transition, the energy and the angular momentum of final state are chosen in accordance with a given actual distributions of probabilities. Accepted transitions are then stored for later use. The procedure is repeated until the sufficient number of transitions is generated. In the following, we analyze results of cascade calculations.

Figure 6 shows a side feeding pattern P_{sf} in per cents, calculated for HFB-200, HFB-600, FM-200 and FM-600 as a function of angular momentum in case of ^{158}Dy . A side feeding is a per cent of the total number of gamma rays which come from 'side' on the yrast line. There are seen three maxima in HFB case. The first one at $10 \hbar$ for 200 and $12 \hbar$ for 600. Other maxima are positioned at $16 \hbar$ and $20 \hbar$. The structure shown for HFB case is generally more complex than in FM calculations. For model 200 (see curve 1) one can see few bumps. These reflect the structure of HFB level densities. Such a structure like this is absent in FM calculations.

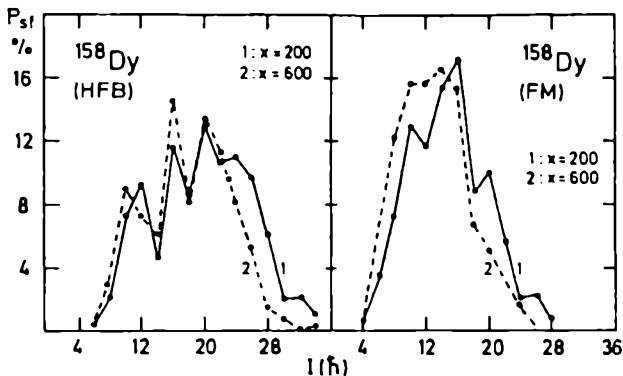


Fig. 6. Side feeding curves for different collective transition strengths x in HFB and Fermi models as a function of angular momentum I . Here x is the parameter in the relation $C_{E1} : C_{M1} : C_{E2} : C_{E2_{coll}} = 50 : 25 : 1 : x$ between electromagnetic transitions strengths constants

Krzywe zasilania boczego dla różnych kolektywnych natężeń x w modelu HFB i modelu Fermiego w funkcji momentu pędu I . Wielkość x jest parametrem w relacji $C_{E1} : C_{M1} : C_{E2} : C_{E2_{coll}} = 50 : 25 : 1 : x$ między stałymi natężeń przejść elektromagnetycznych

Let us analyze now the average energies of gamma quanta emitted in the deexcitation process. We shall look at two kinds of γ -rays: i) collective ($E_{2_{coll}}$ -type) and ii) statistical (other). The energies of both kinds of γ -rays are displayed in Figure 7. Only gamma energies of the '200' model are shown. It is seen that the HFB γ -rays have higher energies than FM γ -rays. The average energy of statistical γ -ray in HFB case is larger than FM average energy on 0.5 MeV. At the same time the average energy of

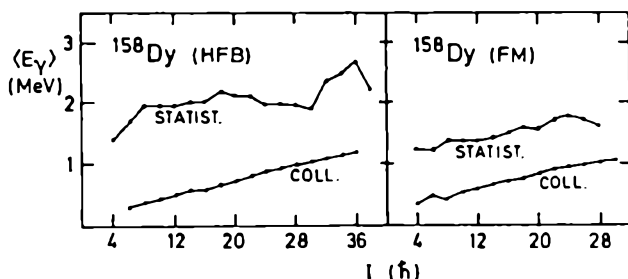


Fig. 7. Average energies of γ -rays in cases of HFB and Fermi model densities
Średnie energie promieniowania γ w przypadku modeli gęstości HFB i Fermiego

collective transitions is comparable for both models and changes linearly from 0.3 MeV at $I = 6$ to 1.1 MeV at $I = 30$.

The average number of gamma transitions at a given angular momentum is called γ -multiplicity (M_γ). Figure 8 shows in its upper part, the total average multiplicities in case of HFB (points) and Fermi model (crosses). In lower part of the figure there are shown corresponding half widths σ of both multiplicity distributions. There is no difference in the shape of the multiplicity function. One can observe that the HFB multiplicity is smaller than the FM with one exception in the region of $I > 22 \hbar$. The corresponding widths are narrower for HFB than for FM model. This picture is consistent with the previously viewed average energies.

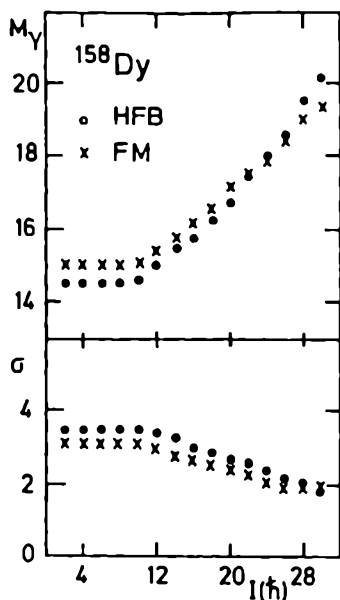


Fig. 8. Multiplicities M_γ and corresponding widths of these distributions σ as a function of angular momentum I in HFB (dots) and Fermi model (crosses) calculations
Wielokrotności M_γ i odpowiadające im szerokości rozkładów σ w funkcji momentu pędu I w modelu HFB (kropki) i modelu FM (krzyżyki)

In Figure 9 there are shown 'side' multiplicities for both considered models. The differences between HFB and FM are better seen here than in the case of total multiplicity. This is connected closely with the differences in level densities as calculated in both models. The difference between both M_γ (HFB and FM) decreases against angular momenta. One observes more (about 2) statistical γ rays in the case of Fermi model in comparison with HFB model and one collective transition more in case of FM. These agree with Figure 7 where we have shown the average energies of gamma transitions. The larger is the multiplicity the smaller is the average transition energy. This remark has a meaning only in the case of statistical gamma rays.

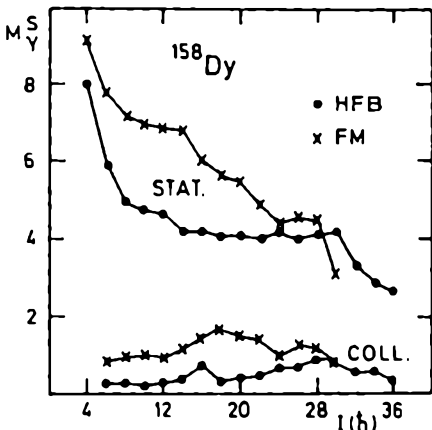


Fig. 9. Side feeding multiplicities of statistical and collective γ -transitions in both HFB (dots) and Fermi (crosses) models

Wielokrotność zasilania z boku przez przejścia γ typu statystycznego oraz kolektywne w obu modelach HFB (kropki) i Fermiego (krzyżyki)

At the end, we compare two final gamma spectra for our reference nucleus ^{158}Dy . These are obtained from both HFB and FM densities. In Figure 10 we show the total spectrum for FM case. One can see the "exponential tail" at higher energies (> 1 MeV) and the small bump at energies smaller than 1 MeV. This bump corresponds to collective transitions. The similar behaviour is seen in Figure 11 where HFB model spectrum has been shown. However, the spectrum at small energies shows the larger bump in this case than in Fermi case model and the energy at which the bump appears is smaller (low energy collective transitions; see Figures 7 and 8). Additionally, at high energies, which are close to 8–9 MeV one can see another rather small hump. We do not know the interpretation of it. It may be simply the effect of pure statistics in cascade calculations.

It will be worthwhile to mention that the HFB gives results which display all the features of experimental spectra.

The whole spectrum of γ radiation from an excited nucleus can be decomposed into the pieces consisting of only elementary multipole γ -rays.

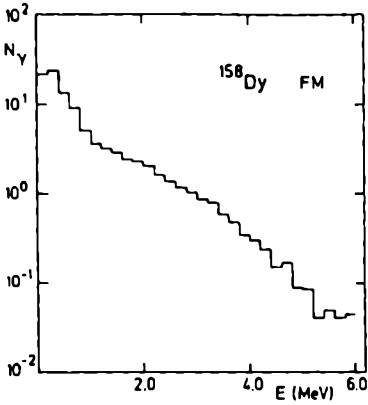


Fig. 10. Gamma spectrum (2000 cascades) for Fermi density model
Widmo gamma otrzymane w modelu Fermiego (2000 kaskad)

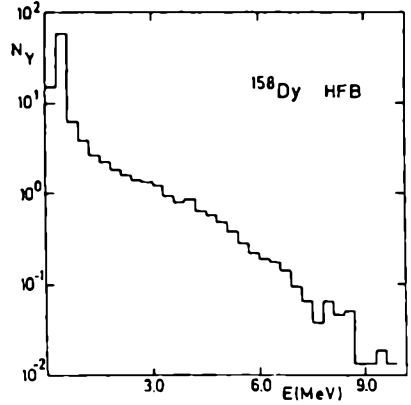


Fig. 11. Gamma spectrum (2000 cascades) for HFB density model
Widmo gamma (2000 kaskad) otrzymane w modelu HFB

Such a decomposition is shown in Figure 12. You can see the collective part $E2_{\text{coll}}$ (dashed line) with maximum around $E_\gamma \sim 0.5$ MeV. The total spectrum in this area consists of the *gamma*-s with this multipolarity. The maximal energies of collective gamma rays achieve 2.5 MeV. The contributions of other γ components exhaust rather high energies. It is remarkable that both $E2$ and $E1$ transitions contribute similar amount to the gamma spectrum at intermediate energies (~ 3 MeV). The tail of the spectrum consists mainly of the $E1$ *gamma*-rays.

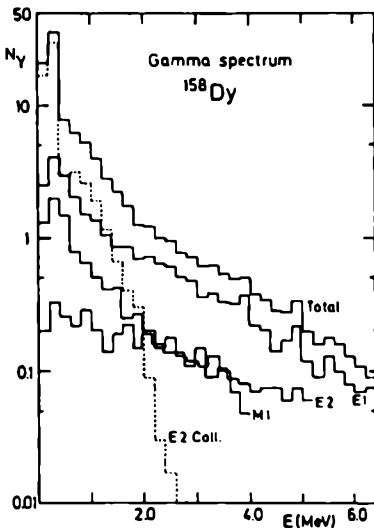


Fig. 12. The decomposed total γ spectrum of the excited ^{158}Dy nucleus. The multipole components of the statistical $E1$, $M1$ and $E2$ as well as the collective component $E2_{\text{coll}}$ are shown

Rozkład szczegółowy pełnego widma γ wzbudzonego jądra ^{158}Dy . Pokazane są wkłady multipolowych statystycznych przejść $E1$, $M1$ i $E2$, jak też kolektywnego przejścia $E2_{\text{coll}}$

REFERENCES

- [1] Diamond R. M., Stephens, F. S., *Ann. Rev. Nucl. Part. Sci.*, 30 (1980) 85.
- [2] Sie S. H., Diamond R. M., Newton J. O. and Leight J. R., *Nucl. Phys.*, A 352 (1981) 279.
- [3] Emling H. et al., *Phys. Lett.*, 98B (1981) 169.
- [4] Grover J. R., Gilat J., *Phys. Rev.*, 157 (1967) 802.
- [5] Gilat J., Grover J. R., *Phys. Rev.*, C 3 (1978) 734.
- [6] Liotta, R. J., Sorensen R. A., *Nucl. Phys.*, A 297 (1978) 136.
- [7] Wakai M., Faessler A., *Nucl. Phys.*, A 307 (1978) 349.
- [8] Leander G., Chen Y. S. and Nilsson B. S., *Phys. Scr.*, 24 (1981) 164.
- [9] Pühlhofer M., *Nucl. Phys.*, A 280 (1977) 264.
- [10] Huizenga J. R., Moretto L. G., *Ann. Rev. Nucl. Sci.*, 22 (1972) 427.
- [11] Mühlshlegel B., *Z. Phys.*, 155 (1959) 313.
- [12] Grossjean M. K., Feldmeier K., *Nucl. Phys.*, A 444 (1985) 113.
- [13] Baranger M., Kumar K., *Nucl. Phys.*, A 62 (1965) 113.
- [14] Baranger M., Kumar K., *Nucl. Phys.*, A 110 (1968) 490.
- [15] Islam S., Mang H. J. and Ring P., *Nucl. Phys.*, A 326 (1979) 161.
- [16] Egido J. L., Mang H. J. and Ring P., *Nucl. Phys.*, A 339 (1980) 390.
- [17] Ring P., Schuck P., *The Nuclear Many Body Problem*, Heidelberg 1980.
- [18] Kamlah A., *Z. Phys.*, 216 (1968) 52.
- [19] Tanabe K., Sugawara-Tanabe K. and Mang H. J., *Nucl. Phys.*, A 357 (1981) 20.
- [20] Sugawara-Tanabe K., Tanabe K. and Mang H. J., *Nucl. Phys.*, A 357 (1981) 45.
- [21] Civitarese O., Schwelling M., *J. Phys. G: Nucl Part. Phys.*, 20 (1994) 1933.
- [22] Hillman M., Grover J. R., *Phys. Rev.*, 185 (1969) 1303.
- [23] Gilat J., *Phys. Rev.*, C 1 (1970) 1432.
- [24] Williams P. C. Jr., Chan, G. and Huizenga, J. R., *Nucl. Phys.*, A 187 (1972) 225.
- [25] Bohr A., Mottelson B. R., *Nuclear Structure*, I, New York 1969.
- [26] Baran A., Dietrich K., *GSI Report*, (1981) 78–79.
- [27] Blatt J.M., Weisskopf V. F., *Theoretical Nuclear Physics*, New York 1952.
- [28] Ring P. et al., *Phys. Lett.*, 110 B (1982) 423.
- [29] Edmonds A. R., *Angular Momentum in Quantum Mechanics*, Princeton 1957.
- [30] Baran A., Dietrich K., *GSI Report*, (1982) 76–77.
- [31] Binder K., [in:] *Monte Carlo Methods in Statistical Physics*, Berlin 1979.
- [32] Binder K., Stanffer D., [in:] *Applications of the Monte Carlo Methods in Statistical Physics*, Berlin 1984.

STRESZCZENIE

W modelu P+QQ jądra atomowego otrzymano gęstości poziomów jądrowych stosując metodę zliczania kwazicząstkowych wzbudzeń, które otrzymano metodą Hartree-Focka-Bogoliubova. Stosując model kaskad otrzymano charakterystyki rozpadu γ jądra atomowego ze stanu wzbudzonego (zadanego w postaci rozkładu wg spinów i energii wzbudzenia) do stanu podstawowego. Uwzględniono przy tym statystyczne przejścia γ typu $E1$, $M1$, $E2$ oraz przejścia kolektywne $E2_{coll}$ („równoległe” do linii *yrast*). Wyniki modelu HFB porównano z wynikami otrzymanymi w modelu gęstości Fermiego.

Oprócz gęstości poziomów jądrowych w pracy podano metodę uśredniania zredukowanych prawdopodobieństw przejść $E1$, $M1$ $E2$ oraz $E2_{coll}$ typu γ . Otrzymane wyniki porównano z tradycyjnymi.